

# A Computational Study of Partially Modified Retro-Inverso Valine Dipeptides: Effect of the Side Chain on the Conformational Preferences of Malonyl and *gem*-Diamino Residues

Carlos Alemán\*

Departament d'Enginyeria Química, E.T.S. d'Enginyers Industrials, Universitat Politècnica de Catalunya, Diagona 647, Barcelona E-08028, Spain

Received: August 2, 2000; In Final Form: October 30, 2000

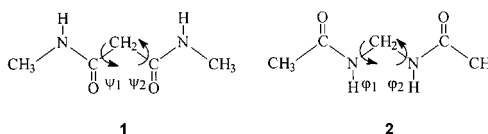
A high-level study of the partially modified retro-inverso compounds derived from valine dipeptide, i.e.,  $\text{CH}_3\text{NHCOCHRCONHCH}_3$  and  $\text{CH}_3\text{CONHCHRNHCOCH}_3$  where  $\text{R} = -\text{CH}(\text{CH}_3)_2$ , is presented. Minimum energy conformations were obtained at the HF/6-31G(d) and MP2/6-31G(d) levels from a systematic conformational analysis. The effects of electron correlation and basis set on relative energies were investigated by performing single point calculations at the HF/6-311G(d,p) and MP2/6-311G(d,p) levels on both HF/6-31G(d) and MP2/6-31G(d) geometries. Furthermore, the influence of polar solvents, i.e., water and methanol, on the conformational preferences of the two compounds was determined using the polarizable continuum model. A comparison with results previously obtained for other partially modified retro-inverso dipeptides promoted an understanding of how the side chain affects the conformational preferences of the malonyl and *gem*-diamino residues.

## Introduction

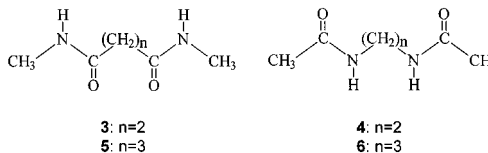
Modified amino acid residues are of relevant interest for their use as building blocks in molecular engineering. They can be used to control the fold of the peptide backbone<sup>1</sup> and to design molecules with enhanced resistance to biodegradation, but the receptor binding ability and biological response of native peptides can be retained.<sup>2</sup> The retro-inverso modification in a peptide chain, i.e., reversal of the direction of the amide bonds, has an important advantage with respect to other modifications: the biological properties of the molecule are influenced without modifying the side chains that could be required for adequate molecular recognition.<sup>3</sup> In a recent work, Fletcher and Campbell reviewed the development of partially modified retro-inverso peptides covering the most significant advances in their synthesis, biological activity, and structure.<sup>4</sup>

Consideration of the impact of partial retro-inverso modification on the residue conformation has prompted much discussion recently.<sup>4,5</sup> Furthermore, the conformational implications associated with such modification can be used to explain the biological behavior of the resulting peptide.<sup>6</sup> Accordingly, computational studies about the preferred conformations of the residues generated by partial retro-inverso modification are highly desirable.

The potential energy surfaces of *N,N'*-dimethylmalonamide<sup>7,8</sup> (**1**) and bis(acetamide)methane<sup>7,9</sup> (**2**), which are partially modified retro-inverso glycine dipeptides, have been investigated using both force-field and quantum mechanical methods. Two minimum energy conformations were located for **1** at both HF/DZP and MP2/DZP levels.<sup>8b</sup> The most stable minimum corresponds to an asymmetric structure with  $\psi_1, \psi_2 = 48.4^\circ, 120.6^\circ$ , stabilized by a six-membered intramolecular hydrogen-bonded ring. Conversely, a single minimum without intramolecular hydrogen bond and  $\varphi_1, \varphi_2 = 69.3^\circ, 67.4^\circ$  has been reported for **2** at the HF/6-31G(d) level.<sup>9</sup>



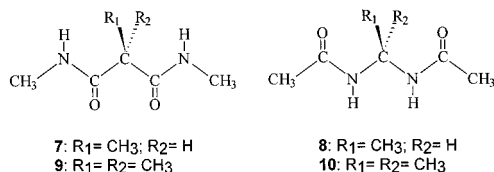
More recently, the conformational impact of adding new methylene units between the two amide groups of **1** and **2** was investigated. This was performed by computing the potential energy surfaces of *N,N'*-dimethylsuccinamide<sup>10</sup> (**3**), *N*-[2-(acetyl amino)ethylene]acetamide<sup>11</sup> (**4**), *N,N'*-dimethylglutaramide<sup>12</sup> (**5**), and *N*-[3-(acetyl amino)propylene]acetamide<sup>11</sup> (**6**), which are partially modified retro-inverso  $\beta$ - and  $\gamma$ -peptides. Their conformational preferences were very different from those predicted for the unmodified peptides.<sup>13</sup> Thus, the malonyl derivatives **3** and **5** are characterized by a gauche conformation for the bond defined by the first and second carbon atoms next to the carbonyl groups.<sup>10,12</sup> On the other hand, a large conformational variability was predicted for the *gem*-diamino derivatives **4** and **6**.<sup>11</sup> Thus, a large number of minima separated by small energy differences were characterized for these compounds. In addition, relative energies strongly depend on the computational level due to the influence of electron correlation.



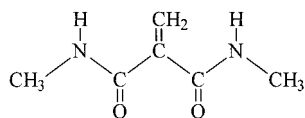
On the other hand, the influence of the side chain on the potential energy surfaces of partially modified retro-inverso peptides was investigated by different authors considering the malonyl and *gem*-diamino derivatives of alanine (**7** and **8**) and  $\alpha$ -amino isobutyric (**9** and **10**) dipeptides.<sup>1a,1b,7,14</sup> However, in all cases these compounds were studied at a low level of theory, i.e., molecular mechanics<sup>1a,7</sup> and semiempirical<sup>1b,14</sup> calculations. The results obtained by the different researchers present serious

\* To whom correspondence should be addressed (E-mail: aleman@eq.upc.es).

discrepancies. Thus, there is a similarity in the conformational maps but the minima are in different positions and of different relative energies. Therefore, it is difficult to understand the effect of the side chain on the conformational preferences of partially modified retro-inverso peptides from these limited studies.

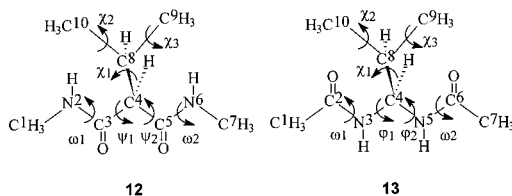


In a recent work, the combination of retro and dehydro modifications was studied by computing the potential energy surface of the malonyl dehydroalanine dipeptide (**11**).<sup>15</sup> These calculations were performed at a high theoretical level and promising results about the applicability of this malonyl residue in peptide design were obtained. However, the side chain modification makes this system too complicated to deduce the general conformational features related to the reversed amide groups in peptides different from **1** and **2**.



11

This work presents an ab initio quantum mechanics study on the partially modified retro-inverso compounds derived from valine dipeptide (**12** and **13**). Valine was selected as parent residue by two reasons: (1) It presents a higher percentage of occurrence in proteins than other residues;<sup>16</sup> and (2) the X-ray-determined structures of dipeptides containing the corresponding malonyl and *gem*-diamino residues are available in the literature.<sup>17–20</sup> The minimum energy conformations located for **12** and **13** have been compared with those reported for other partially modified retro-inverso dipeptides. Results have allowed us to understand how the side chain affects the conformational preferences of malonyl and *gem*-diamino residues. Furthermore, the effects of polar solvents on the conformational preferences of **12** and **13** have been investigated.



## Methods

The conformational spaces of compounds **12** and **13** were systematically explored in order to characterize all of the minimum energy conformations. Because each flexible dihedral angle is expected to have 3 minima,  $3^5 = 243$  minima may be anticipated for the potential energy hypersurfaces  $E = E(\psi_1, \psi_2, \chi_1, \chi_2, \chi_3)$  and  $E = E(\varphi_1, \varphi_2, \chi_1, \chi_2, \chi_3)$ . However, each of the two methyl groups have three degenerate torsional minima, allowing the number of theoretical minima to be reduced. Thus, the potential energy hypersurfaces of **12** and **13** can be described effectively with three independent torsional variables, i.e.,  $E = E(\psi_1, \psi_2, \chi_1)$  and  $E = E(\varphi_1, \varphi_2, \chi_1)$  respectively, when  $\chi_2$  and  $\chi_3$  are optimized but nominally  $\chi_2 = \chi_3 = 60^\circ$ .<sup>21</sup> Furthermore,

**TABLE 1: Minima<sup>a</sup> Obtained from HF/6-31G(d) and MP2/6-31G(d) Geometry Optimizations for **12****

no.	$\omega_1$	$\psi_1$	$\psi_2$	$\omega_2$	$\chi_1$
HF/6-31G(d)					
<b>12a</b>	-177.6	53.0	112.1	-178.1	-176.3
<b>12b</b>	178.4	-126.7	-22.8	-176.9	-59.7
<b>12c</b>	179.4	30.1	134.5	177.7	-69.8
<b>12d</b>	172.7	-66.0	116.7	174.3	169.4
<b>12e</b>	174.7	85.0	-46.2	176.9	-179.1
MP2/6-31G(d)					
<b>12a</b>	-177.6	52.4	116.9	-179.3	-176.6
<b>12b</b>	-176.3	-130.1	-24.0	-175.6	-57.5
<b>12c</b>	-179.2	35.0	136.9	178.2	-64.4
<b>12d</b>	171.9	-62.8	106.5	174.7	169.3
<b>12e</b>	173.7	80.2	-44.4	177.5	-177.1

<sup>a</sup> Dihedral angles in degrees.

because of the molecular symmetry of these compounds, the  $3^3 = 27$  theoretical minima, can be reduced to 14, i.e.,  $\varphi_1, \varphi_2 = -\varphi_1, -\varphi_2$  and  $\psi_1, \psi_2 = -\psi_1, -\psi_2$  for **12** and **13**, respectively. All of these structures were taken as starting points in HF/6-31G(d)<sup>22</sup> geometry optimizations. Frequency analyses were performed to verify the nature of minimum energy state of the stationary points located during geometry optimizations as well as to obtain zero-point energies (ZPEs), thermal corrections, and entropies. To explore the effects of electron correlation on molecular geometries, the structures resulting from HF/6-31G(d) optimizations were used as starting points for full optimization at the MP/6-31G(d) level.<sup>23</sup> The resulting residual Cartesian gradients were less than  $3 \cdot 10^{-4}$  hartree/bohr. Single point calculations at the HF/6-311G(d,p) and MP2/6-311G(d,p) level were performed on optimized structures.

Solvent effects on the conformational preferences of **12** and **13** were investigated using the polarizable continuum model (PCM).<sup>24</sup> This model represents the polarization of the liquid by a charge density appearing on the surface of the cavity created in the solvent. This cavity is built using a molecular shape algorithm. PCM calculations were performed at the HF/6-311G(d,p) level using the standard protocol and considering two dielectric constants:  $\epsilon = 78.4$  for H<sub>2</sub>O and  $\epsilon = 33.0$  for CH<sub>3</sub>OH.

All of the calculations were performed with the Gaussian 98<sup>25</sup> computer program. Calculations were run on an IBM/SP2 at the Centre de Supercomputació de Catalunya (CESCA).

## Results and Discussion

**Conformational Preferences of Partially Modified Retro-Inverso Valine Dipeptides.** The dihedral angles of the minimum energy conformations obtained from HF/6-31G(d) and MP2/6-31G(d) geometry optimizations on **12** and **13** are displayed in Tables 1 and 2, respectively, whereas the relative enthalpies are listed in Tables 3 and 4.

For compound **12**, five minima were located, as shown in Figure 1. All of these conformations are stabilized by intramolecular hydrogen bonds between the two amide groups, the hydrogen bonding parameters being also displayed in Figure 1. At each level of calculation, conformer **12a** is predicted to be the most stable. In this conformer, dihedral angles  $\psi_1$  (52.4°) and  $\psi_2$  (116.9°) are close to those predicted for the minimum energy conformation of **1**,<sup>8</sup> while dihedral angle  $\chi_1$  (-176.6°) is trans. Thus, conformer **12a** forms an intramolecular six-membered hydrogen-bonded ring, denoted C<sub>6</sub>, involving the NH and C=O moieties of different amide groups. This structural pattern was also found for **1**. Conformer **12c** can be derived from **12a** by rotating the dihedral angle  $\chi_1$  from trans to gauche.

**TABLE 2: Minima<sup>a</sup> Obtained from HF/6-31G(d) and MP2/6-31G(d) Geometry Optimizations for 13**

no.	$\omega_1$	$\varphi_1$	$\varphi_2$	$\omega_2$	$\chi_1$
HF/6-31G(d)					
13a	-170.5	54.3	75.7	-169.7	-174.3
13b	169.7	-92.6	-39.6	172.0	61.6
13c	-172.3	37.8	92.6	-169.3	68.1
13d	-172.8	-83.3	152.5	-165.4	-67.2
13e	-170.2	-70.9	125.3	-160.1	65.2
13f	-174.2	-76.1	129.7	-162.3	172.8
13g	171.9	54.1	-95.2	155.3	-170.7
13h	-156.3	93.1	-42.6	-172.0	49.4
MP2/6-31G(d)					
13a	-167.7	52.8	69.8	-171.8	-175.1
13b	172.4	-99.2	-38.5	172.3	60.1
13c	-175.5	38.0	116.2	-175.8	62.7
13d	-171.7	-81.5	153.6	-163.9	-66.0
13e	-169.0	-71.3	123.9	-156.5	62.3
13f	-172.8	-73.9	127.3	-158.3	173.3
13g	170.1	59.3	-93.3	151.6	-172.7
13h	-152.7	91.3	-48.5	-170.5	-48.3

<sup>a</sup> Dihedral angles in degrees.**TABLE 3: Relative Enthalpies<sup>a</sup> for 12**

level <sup>b</sup>	12a	12b	12c	12d	12e
HF/6-31G(d)//HF/6-31G(d)	0.0 <sup>c</sup>	1.4	1.7	5.0	7.2
HF/6-311G(d,p)//HF/6-31G(d)	0.0 <sup>d</sup>	1.3	1.7	4.8	7.0
MP2/6-311G(d,p)//HF/6-31G(d)	0.0 <sup>e</sup>	1.3	1.5	4.7	6.0
MP2/6-31G(d)//MP2/6-31G(d)	0.0 <sup>f</sup>	1.3	1.5	5.6	6.6
HF/6-311G(d,p)//MP2/6-31G(d)	0.0 <sup>g</sup>	1.4	1.8	4.9	7.2
MP2/6-311G(d,p)//MP2/6-31G(d)	0.0 <sup>h</sup>	1.3	1.7	4.8	6.0

<sup>a</sup> In units of kcal/mol. Zero point energies and thermal corrections computed at the HF/6-31G(d) level are included. <sup>b</sup> Level of energy calculation/level of geometry optimization. <sup>c</sup>  $E = -570.647911$  au. <sup>d</sup>  $E = -571.795644$  au. <sup>e</sup>  $E = -572.713588$  au. <sup>f</sup>  $E = -572.366668$  au. <sup>g</sup>  $E = -571.787842$  au. <sup>h</sup>  $E = -572.717885$  au.

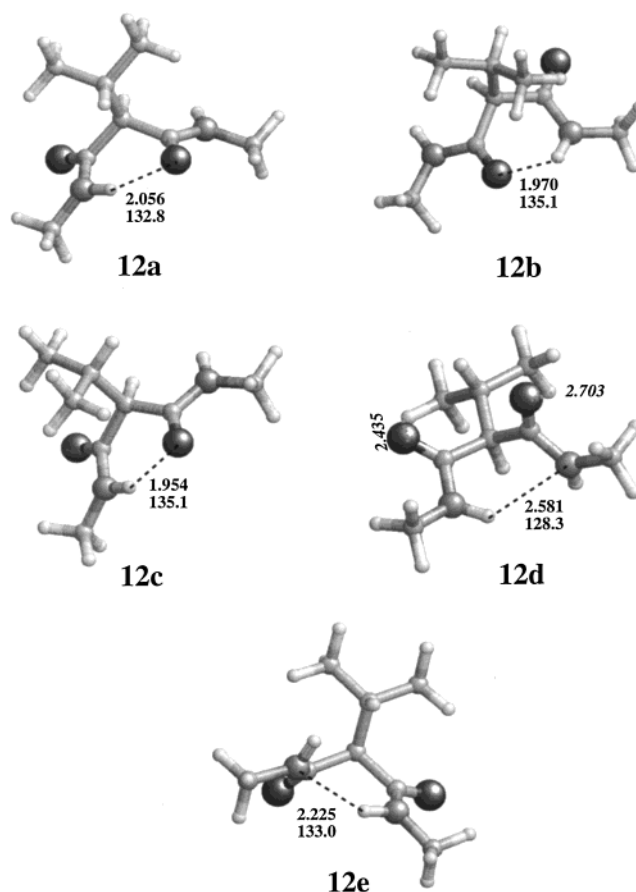
This side chain conformation is preserved in conformer **12b** but both the sign and the values of the backbone dihedral angles are exchanged with respect to those in **12c**, i.e.,  $-\psi_2$ ,  $-\psi_1$ . Both conformers **12b** and **12c** form C<sub>6</sub> hydrogen-bonded structures. Despite the strong hydrogen bond in these conformers, they are less stable than **12a** by 1.3 and 1.7 kcal/mol, respectively, at the best level of theory (Table 3). The major reason that **12a** is more stable than **12b** and **12c** is the former's favorable dihedral angle  $\chi_1$ . Thus, inductive forces (dipole-induced dipole interaction) are  $\chi_1$  dependent.<sup>26</sup> The modulation of induction to the intramolecular energy is analyzed in Table 5 using the Mulliken charges. The variation of the charges with  $\chi_1$  explains the largest induced dipole moment and the overall stabilization of the conformer **12a** with respect to **12b** and **12c**. The effect of the induction in the stability of the conformers with  $\chi_1 \approx$  trans with respect to those with  $\chi_1 \approx$  gauche was previously described for the formyl-L-valinamide.<sup>26</sup>

Both conformers **12d** and **12e** also form a C<sub>6</sub> structure but with intramolecular hydrogen bonds set between the NH

**TABLE 4: Relative Enthalpies<sup>a</sup> for 13**

level <sup>b</sup>	13a	13b	13c	13d	13e	13f	13g	13h
HF/6-31G(d)//HF/6-31G(d)	0.0 <sup>c</sup>	2.4	2.5	3.0	3.7	3.8	11.0	14.8
HF/6-311G(d,p)//HF/6-31G(d)	0.0 <sup>d</sup>	2.4	2.5	2.7	3.6	3.6	11.1	14.8
MP2/6-311G(d,p)//HF/6-31G(d)	0.0 <sup>e</sup>	2.2	2.4	3.0	3.2	3.3	9.6	13.5
MP2/6-31G(d)//MP2/6-31G(d)	0.0 <sup>f</sup>	2.1	2.1	3.5	3.6	3.8	9.7	13.3
HF/6-311G(d,p)//MP2/6-31G(d)	0.0 <sup>g</sup>	2.8	2.6	2.6	3.7	3.6	11.2	14.9
MP2/6-311G(d,p)//MP2/6-31G(d)	0.0 <sup>h</sup>	2.2	2.2	3.0	3.0	3.2	9.4	13.2

<sup>a</sup> In units of kcal/mol. Zero point energies and thermal corrections computed at the HF/6-31G(d) level are included. <sup>b</sup> Level of energy calculation/level of geometry optimization. <sup>c</sup>  $E = -570.659319$  au. <sup>d</sup>  $E = -571.083364$  au. <sup>e</sup>  $E = -572.997546$  au. <sup>f</sup>  $E = -572.650009$  au. <sup>g</sup>  $E = -571.075718$  au. <sup>h</sup>  $E = -573.001134$  au.

**Figure 1.** Minimum energy conformations of **12** obtained at the MP2/6-31G(d) level.

moieties of the two amide bonds. They are 4.8 and 6.0 kcal/mol less stable, respectively, less stable than the global minimum. These results indicate that the N-H...N interaction is less attractive than the N-H...O interaction. Thus, the hydrogen atoms of the amide groups, which are positively charged, are very close in the space inducing an increase in the H...N distance with respect to the H...O distance.

The structure of **12** was determined by X-ray crystallography.<sup>20</sup> It consists of a semiextended conformation with  $\psi_1 = -\psi_2 = -110.4^\circ$  and  $\chi_1 = 178.1^\circ$ . The two amide groups are hydrogen bonded with the neighboring molecule in such a way as to form a parallel  $\beta$ -sheet structure. This structure does not correspond to any of the minimum energy conformations predicted for **12** in the gas phase (Table 1). Thus, the presence of two hydrogen bonds has not been introduced in our theoretical calculations. In the crystallized compound the optimal conformation appears when infinite networks of hydrogen bonds are formed rather than an isolated intramolecular hydrogen bond such as in the gas phase. On the other hand, IR and NMR studies<sup>27</sup> indicated that small peptides constituted by a malonyl

**TABLE 5: Mulliken Population Analysis of the Side Chain Atoms for Conformers 12a, 12b, 12c, 13a, 13b, and 13c**

no.	12a	12b	12c	13a	13b	13c
C8	-0.2084	-0.1557	-0.1659	-0.1842	-0.1368	-0.1362
H(-C8)	0.2082	0.1669	0.1033	0.2035	0.1736	0.1499
C9H <sub>3</sub>	0.0340	0.035	0.0860	0.0142	-0.0040	0.0187
C10H <sub>3</sub>	0.0150	0.0101	0.0990	0.0158	0.0190	0.0177

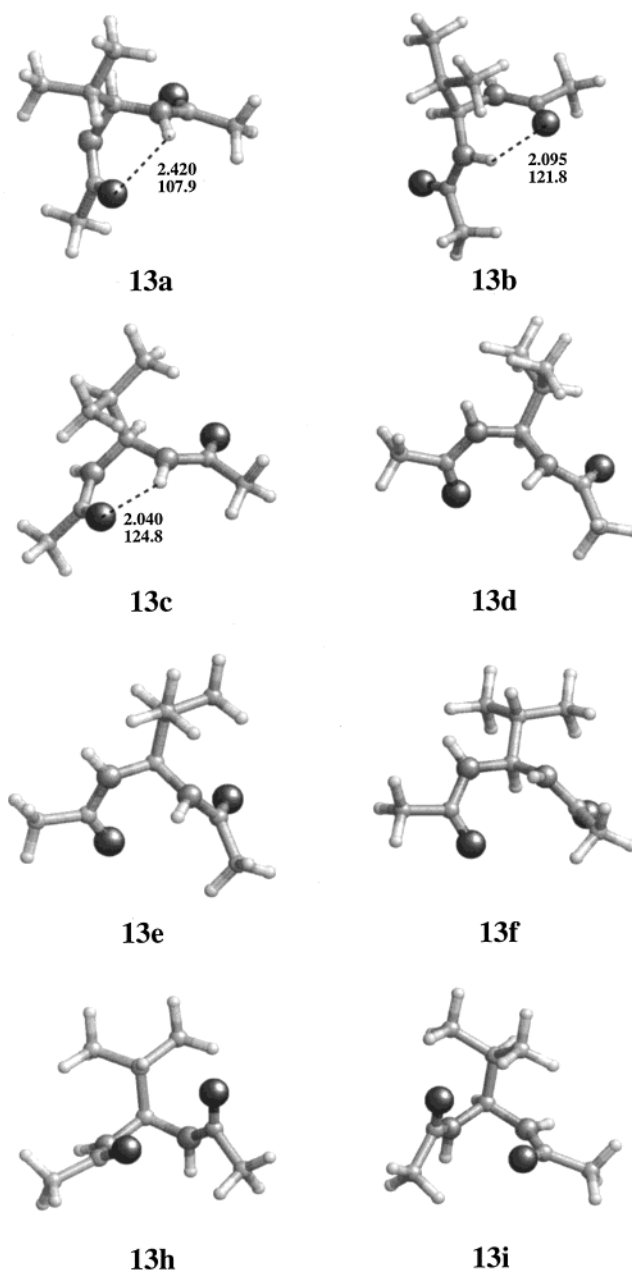
residue tend to adopt a C<sub>6</sub> structure in solution, as is predicted from the theoretical calculations.

Figure 2 shows the eight conformational minima characterized for compound **13**. The main difference between conformers **13a** and **13c**, which form a C<sub>6</sub> structure, is dihedral angle  $\chi_1$ . The latter clearly presents a better hydrogen bonding geometry than the former. However, conformer **13a** is more stable than **13c** by 2.2 kcal/mol. Conformer **13b** also presents a C<sub>6</sub> structure and is 2.2 kcal/mol less stable than the global minimum. The stabilization of **13a** with respect to **13b** and **13c** is explained by the effect of isopropyl side group on electron distribution. Thus, as was discussed above for compound **12** and previously for formyl-L-valinamide,<sup>26</sup> the conformers with  $\chi_1 \approx \text{trans}$  are stabilized with respect to those with  $\chi_1 \approx \text{gauche}$  by the inductive forces. Table 5 lists the Mulliken charges obtained for the isopropyl side group in conformers **13a**, **13b**, and **13c**. As can be seen, the largest separation of charges is obtained for the former conformer.

Conformers **13d**, **13e**, and **13f** are quite similar. The three conformers can be interconverted by the rotation of the dihedral angle  $\chi_1$ . They are predicted to be about 3.0–3.2 kcal/mol higher in energy than **13a**. Note that they are stabilized by a favorable arrangement of the amide dipoles rather than by an intramolecular hydrogen bond. Finally, conformers **13g** and **13h** are 9.4 and 13.2 kcal/mol less stable than **13a**, apparently due to the large electrostatic repulsion between the two amide dipoles. Thus, in these conformers the oxygen atom of one amide group points to the negatively charged atoms of the second amide group, i.e. the oxygen and nitrogen atoms.

The structure of **13** was determined by Kemme et al.<sup>17</sup> 20 years ago using X-ray crystallography. The dihedral angles of the resulting conformation were  $\varphi_1, \varphi_2 = 113^\circ, -105^\circ$ . On the other hand, the structures of two related molecules also have been also reported.<sup>18,19</sup> Such compounds only differ from **13** in the end alkyl groups. Thus, the (CH<sub>3</sub>)<sub>2</sub>N-CO<sup>18</sup> and (CH<sub>3</sub>)<sub>3</sub>C-CO<sup>19</sup> moieties replaced the end acetyl groups. However, the influence of these modifications in the backbone conformation is quite small, i.e.,  $\varphi_1, \varphi_2 = 105^\circ, -124^\circ$ <sup>18</sup> and  $\varphi_1, \varphi_2 = 101^\circ, -99^\circ$ ,<sup>19</sup> respectively. Thus, in all cases the molecules present a semiextended conformation with intermolecular hydrogen bonds arranged as in a parallel  $\beta$ -sheet structure. Furthermore, the side chain adopts a trans conformation with  $\chi_1 \approx 180^\circ$  in the three crystallized compounds. As can be seen in Table 2, the observed conformation does not correspond to an energy minimum, **13f** being the closest structure ( $\Delta\varphi_1, \Delta\varphi_2, \Delta\chi_1 = 39^\circ, 22^\circ, 5^\circ$ ).

Tables 1 and 2 compare the conformational dihedral angles obtained at the HF/6-31G(d) and MP2/6-31(d) levels. It is worth noting that the structures obtained at the MP2 level are quite consistent with those determined from HF calculations. For **12** and **13** the largest difference corresponds to the dihedral angles  $\psi_2$  of **12d** (10.2°) and  $\varphi_2$  of **13c** (23.6°), respectively. On the other hand, relative enthalpies displayed in Table 3 indicate that the effects associated with the size of the basis set and electron correlation are very small for **12**. Thus, the average difference between the relative enthalpies predicted at the highest and lowest levels of theory, i.e., MP2/6-311G(d,p)//MP2/6-31G(d) and HF/6-31G(d)//HF/6-31G(d), respectively, is only

**Figure 2.** Minimum energy conformations of **13** obtained at the MP2/6-31G(d) level.

0.3 kcal/mol. This average difference increases to 0.7 kcal/mol for **13**. Thus, inspection of Table 4 shows that the level of theory plays a more important role in the relative enthalpies predicted for **13**. The influence of the basis set is considerably small, as occurs for compound **12**. Thus, the average difference between the relative enthalpies computed with the 6-31G(d) and 6-311G(d,p) basis sets ranges from 0.1 to 0.3 kcal/mol depending on the level of geometry optimization. However, the effect of electron correlation is quite important and needs to be taken into account. The average difference between the relative enthalpies computed at the MP2/6-311G(d,p)//MP2/6-31G(d) and HF/6-311G(d,p)//MP2/6-31G(d) levels is 0.8 kcal/mol.

Tables 6 and 7 provide a comparison of geometric parameters obtained at the MP2/6-31G(d) level with experimental values for **12** and **13**, respectively. The experimental bond lengths and angles of **12** are well reproduced by MP2 calculations with standard deviations in the unsigned differences of 0.017 Å and 1.7°, respectively. For **13** the comparison with experiment is more difficult because the final agreement factor *R* for the three



**TABLE 6: Optimized MP2/6-31G(d) Geometries<sup>a</sup> for 12**

parameter	12a	12b	12c	12d	12e	X-ray <sup>b</sup>
C1–N2	1.451	1.453	1.451	1.454	1.459	1.445
N2–C3	1.358	1.356	1.352	1.367	1.384	1.322
C3–C4	1.530	1.516	1.530	1.537	1.524	1.514
C3=O	1.236	1.245	1.239	1.231	1.231	1.230
C4–C5	1.518	1.531	1.518	1.523	1.532	1.514
C5=O	1.242	1.238	1.244	1.231	1.234	1.230
C5–N6	1.357	1.352	1.357	1.376	1.364	1.322
N6–C7	1.452	1.450	1.453	1.457	1.453	1.445
C4–C8	1.544	1.553	1.557	1.533	1.545	1.530
C8–C9	1.527	1.527	1.527	1.528	1.530	1.511
C9–C10	1.528	1.528	1.528	1.529	1.529	1.511
C1–N2–C3	120.3	120.8	120.0	119.8	118.3	122.9
N2–C3–C4	114.7	115.5	116.8	113.8	116.3	116.7
C3–C4–C5	111.3	115.4	115.0	106.1	112.1	108.9
C4–C5–N6	115.6	117.1	115.0	115.3	116.1	116.7
C5–N6–C7	122.4	120.3	120.7	119.3	119.5	122.9
N2–C3=O	123.7	120.8	123.0	122.6	121.2	121.4
C4–C5=O	121.5	119.4	124.1	122.2	121.2	121.8
C3–C4–C8	111.0	111.6	111.7	112.7	110.2	111.9
C4–C8–C9	110.8	113.0	113.1	110.8	110.2	111.1
C4–C8–C10	110.5	111.0	110.6	110.7	111.2	111.1

<sup>a</sup> Distances and angles in angstroms and degrees, respectively. <sup>b</sup> From Reference 20.

compounds containing the *gem*-diamino residue was too large.<sup>17–19</sup> Table 7 lists the geometric parameters of the structure determined with a lowest *R* factor (*R* = 8.1%): <sup>t</sup>BuCO–NHCH(<sup>i</sup>Pr)NH–CO<sup>t</sup>Bu.<sup>19</sup> Nevertheless, experimental parameters present significant deformations in the various groups that constitute the molecule precluding a quantitative comparison with the theoretical values. For instance, the C–CH<sub>3</sub> bond lengths of the isopropyl side group are extremely short, i.e., about 0.07 Å with respect to the standard value. On the other hand, the geometric parameters obtained at the HF/6-31G(d) level (data not show) were compared with the MP2/6-31G(d) parameters of Tables 6 and 7, providing standard deviations of 0.012 Å and 0.7° (12) and 0.011 Å and 0.8° (13).

**Effect of the Solvent.** Tables 8 and 9 list the free energies ( $\Delta G$ ) at *T* = 298 K in the gas phase, methanol solution, and aqueous solution for 12 and 13, respectively. Free energies in the gas phase were computed using the relative enthalpies estimated at the MP2/6-311G(d,p)/MP2/6-31G(d) level (Tables 3 and 4) and the entropies computed at the HF/6-31G(d) level.

**TABLE 7: Optimized MP2/6-31G(d) Geometries<sup>a</sup> for 13**

parameter	13a	13b	13c	13d	13e	13f	13g	13h	X-ray <sup>b</sup>
C1–C2	1.514	1.514	1.515	1.514	1.514	1.514	1.517	1.514	1.507
C2–N3	1.369	1.376	1.362	1.374	1.375	1.373	1.373	1.385	1.343
C2=O	1.237	1.233	1.240	1.231	1.231	1.231	1.232	1.227	1.229
N3–C4	1.465	1.443	1.468	1.444	1.454	1.449	1.469	1.454	1.452
C4–N5	1.451	1.471	1.443	1.466	1.459	1.461	1.455	1.471	1.444
N5–C6	1.376	1.363	1.370	1.372	1.381	1.378	1.388	1.373	1.345
C6–C7	1.513	1.515	1.514	1.513	1.511	1.512	1.515	1.517	1.485
C6=O	1.234	1.239	1.234	1.234	1.230	1.231	1.227	1.232	1.234
C4–C8	1.532	1.534	1.536	1.532	1.532	1.531	1.533	1.541	1.520
C8–C9	1.527	1.523	1.528	1.527	1.527	1.530	1.529	1.527	1.46
C8–C10	1.528	1.526	1.526	1.527	1.528	1.526	1.527	1.528	1.44
C1–C2–N3	115.2	114.2	115.2	115.0	115.0	115.1	114.4	113.0	120.1
C2–N3–C4	120.5	120.2	125.2	121.2	120.3	121.0	124.2	129.0	125.3
O=C2–N3	122.4	123.0	121.4	121.9	121.9	123.1	122.4	122.0	120.4
N3–C4–N5	111.6	111.4	110.8	108.7	108.8	108.7	109.8	110.4	108.7
C4–N5–C6	118.3	124.5	120.9	118.9	118.8	119.2	126.6	125.9	126.1
N5–C6–C7	114.9	115.1	114.5	115.2	114.7	114.8	113.2	114.1	118.8
N5–C6=O	122.0	123.2	123.0	121.7	122.1	122.1	124.6	123.9	118.6
N3–C4–C8	112.7	112.7	112.8	111.5	110.5	110.2	113.7	118.8	110.7
C4–C8–C9	110.4	110.0	109.2	112.7	109.6	110.6	109.3	116.2	108.9
C4–C8–C10	110.0	114.4	113.8	110.8	112.2	110.3	110.1	111.0	109.7

<sup>a</sup> Distances and angles in angstroms and degrees, respectively. <sup>b</sup> From reference 19.

Free energies in solution are based on enthalpies in solution and entropies in the gas phase. Enthalpies in solution were estimated by adding the solvent effects obtained with PCM at the HF/6-311G(d,p)/MP2/6-31G(d) level, i.e.,  $\Delta(E_{\text{sol}} - E_{\text{gas}})$ , to enthalpies in the gas phase.

Table 8 shows that for 12 the energy order of the minimum energy conformations is not modified by solvation. Thus, the conformational preferences of 12 in solution remain essentially unaltered with respect to those of the gas phase. The largest change in  $\Delta G$  corresponds to the highest energy conformer 12e, which is stabilized by 3.2 and 2.4 kcal/mol in aqueous and methanol solutions, respectively. Conversely, the solvent has a dramatic influence on the conformational preferences of 13. Thus, water and methanol introduce important changes in the relative energy order of the minimum energy conformations of 13. Polar solvents stabilize conformers 13d, 13e, and 13f by about 2.7–3.2 kcal/mol. Thus, 13f is predicted to be the most stable conformation in solution, conformers 13e and 13d being only 0.3 and 0.8 kcal/mol less favored, respectively. In solution, conformer 13a, which was the lowest energy minimum in the gas phase, is about 0.8–0.9 kcal/mol less stable than 13f.

The magnitude of the polarization effects provided by water and methanol solvents has been estimated by determining the solvent-induced dipole factor for the two compounds. Accordingly, dipole moments computed in the gas-phase at the HF/6-311(d,p) level have been compared by a linear regression analysis ( $y = cx$ ) with those obtained in solution at the same level of theory. The linear correlation coefficient *r* was larger than 0.99 for the two solvents. The slope of the linear regression function *c* was 1.39 and 1.35 for water and methanol, respectively. Thus, water and methanol increase the dipole moment by 39% and 35%, respectively, over gas-phase values. Although the dielectric constant of water is much higher than that of methanol, the changes induced by the two polar solvents are very similar.

**Effect of the Side Chain in the Conformational Preferences of Partially Modified Retro-Inverso Dipeptides.** Tables 10 and 11 compare the backbone dihedral angles of the lowest energy minimum predicted at different quantum mechanical levels for dipeptides containing malonyl and *gem*-diaminoalkyl residues, respectively. As can be seen, results indicate that the conformational preferences of the two types of retro-inverso

**TABLE 8: Relative Free Energies<sup>a</sup> (*T* = 298 K) in the Gas Phase<sup>b</sup> and in Methanol and Aqueous Solutions<sup>c</sup> for **12****

environment	12a	12b	12c	12d	12e
gas phase	0.0	1.4	1.7	5.2	6.6
methanol solution	0.0	1.0	2.3	3.1	4.2
aqueous solution	0.0	1.0	2.4	3.0	3.4

<sup>a</sup> In units of kcal/mol. <sup>b</sup> Relative enthalpy at the MP2/6-311G(d,p)//MP2/6-31G(d) level (Table 3) and entropy at the HF/6-31G(d) level.

<sup>c</sup> Gas-phase enthalpy MP2/6-311G(d,p)//MP2/6-31G(d) level, solvent effect at the HF/6-311G(d,p)//MP2/6-31G(d) level, and entropy at the HF/6-31G(d) level.

**TABLE 9: Relative Free Energies<sup>a</sup> (*T* = 298 K) in the Gas Phase<sup>b</sup> and in Methanol and Aqueous Solutions<sup>c</sup> for **13****

environment	13a	13b	13c	13d	13e	13f	13g	13h
gas phase	0.0	2.3	2.3	3.1	3.7	3.2	10.7	14.6
methanol solution	0.8	2.1	1.7	0.3	0.8	0.0	8.5	13.9
aqueous solution	0.9	2.2	1.8	0.3	0.8	0.0	8.4	13.1

<sup>a</sup> In units of kcal/mol. <sup>b</sup> Relative enthalpy at the MP2/6-311G(d,p)//MP2/6-31G(d) level (Table 3) and entropy at the HF/6-31G(d) level.

<sup>c</sup> Gas-phase enthalpy at the MP2/6-311G(d,p)//MP2/6-31G(d) level, solvent effect at the HF/6-311G(d,p)//MP2/6-31G(d) level, and entropy at the HF/6-31G(d) level.

**TABLE 10: Predicted Global Minimum<sup>a</sup> for Malonyl Residues**

compound	$\psi_1$	$\psi_2$	level of theory	ref
<b>1</b>	48.4	120.6	MP2/DZP	8b
	47.5	108.3	HF/4-31G(d)	8a
	52.7	111.5	AM1	8a
<b>7</b>	55.0	112.5	AM1	14
<b>9</b>	53.4	103.2	AM1	14
<b>11</b>	13.2	142.5	HF/6-31+G(d,p)	15
	13.0	143.8	HF/6-31G(d)	15
	13.3	146.8	HF/4-31G	15
<b>12</b>	52.4	116.9	MP2/6-31G(d)	present work
	53.0	112.1	HF/6-31G(d)	present work

<sup>a</sup> Dihedral angles in degrees.

**TABLE 11: Predicted Global Minimum<sup>a</sup> for *gem*-Diaminoalkyl Residues**

compound	$\varphi_1$	$\varphi_2$	level of theory	reference
<b>2</b>	69.3	66.9	HF/6-31G(d)	9
	72.5	70.8	HF/3-21G	9
	69.3	67.4	AM1	9
<b>8</b>	72.0	59.9	HF/3-21G	14
	66.2	58.2	AM1	1b
	55.8	55.8	AM1	1b
<b>13</b>	52.8	69.8	MP2/6-31G(d)	present work
	54.3	75.7	HF/6-31G(d)	present work

<sup>a</sup> Dihedral angles in degrees.

residues are not influenced by size of the side group. Thus, the backbone conformations of the global minimum remain unaltered as the side group goes from H through CH<sub>3</sub> to CH(CH<sub>3</sub>)<sub>2</sub>.

On the other hand, the influence of the side group on the complete potential energy surfaces of retro-inverso residues has been investigated by comparing all the minima predicted for compounds listed in Tables 10 and 11. For malonyl residues, it can be stated that the side group does not induce the creation of a new type of backbone conformation. Thus, all the backbone minima computed for **7**, **9**, and **12** are close to the two minima found for **1** at a similar level of theory.<sup>8a</sup> It should be emphasized that the deviations found in the dihedral angles  $\psi_1$  and  $\psi_2$  of **11** with respect to the other compounds listed in Table 10 are due to the geometric restrictions imposed by the sp<sup>2</sup> carbon atom. A different behavior is observed for *gem*-diaminoalkyl residues. Thus, when the hydrogen side group of **2** is replaced

by CH<sub>3</sub> or CH(CH<sub>3</sub>)<sub>2</sub>, a new type of backbone minimum appears at  $\varphi_1$ ,  $\varphi_2 \approx -70^\circ$ ,  $125^\circ$ . This is induced by the unfavorable interactions between the backbone and the side chain associated with the loss of molecular symmetry. Thus, the minimum of **2**, which is 4-fold degenerated, changes to two 2-fold degenerated minima.

## Conclusions

This paper presents a detailed ab initio study of the conformational preferences of the partially modified retro-inverso valine dipeptides **12** and **13**. The results include a detailed investigation of the minimum energy conformations of the two compounds at the HF/6-31G(d) and MP2/6-31G(d) levels of theory. Furthermore, single point calculations were performed in the gas phase at the HF/6-311G(d,p) and MP2/6-311G(d,p) levels and in methanol and aqueous solutions at the HF/6-311G(d,p) level. The principal conclusions obtained from these results are as follows.

Optimized structures obtained at the HF/6-31G(d) level are in generally good agreement with the MP2/6-31G(d) results, the influence of electron correlation on the molecular geometries of the two compounds being small. These results suggest that the HF level is a reliable choice for geometry optimizations on retro-peptide conformers. A similar conclusion was reached by a number of authors for other amino acids.<sup>28</sup> On the other hand, the effect of the basis set on the relative energies is very small, i.e., less than 0.3 kcal/mol. Conversely, the effects of electron correlation in relative energies are different in **12** and **13**. Thus, electron correlation plays an almost negligible role in the former, whereas a significant influence was detected in the latter. In view of these results, it appears that the MP2/6-311G(d,p)//HF/6-31G(d) is a suitable level of theory to describe the conformational preferences of partially modified retro-inverso peptides.

The lowest energy conformation of **12** in the gas phase, methanol solution, and aqueous solution corresponds to a C<sub>6</sub> backbone orientation with a trans conformation in the side chain. A similar structure was also the most stable for **13** in the gas phase. However, in solution it becomes almost 1 kcal/mol less favored than a conformation without intramolecular hydrogen bond. The most remarkable difference between the potential energy hypersurfaces of **12** and **13** is that all the minimum energy conformations of the former are stabilized by intramolecular hydrogen bonds, whereas the latter presents five minima without such interaction.

The conformational analyses reported here together with those previously reported for other partially modified retro-inverso dipeptides have revealed that the side chain has a small influence on the backbone conformations of malonyl and *gem*-diamino residues. We are currently using the present results together with additional ab initio calculations to derive an improved parameter set for a retro-peptides force field.

**Acknowledgment.** The author is indebted to the Centre de Supercomputació de Catalunya (CESCA) for computational facilities.

## References and Notes

- (1) (a) Dauber-Osguthorpe, P.; Campbell, M. M.; Osguthorpe, D. J. *Int. J. Pept. Protein Res.* **1991**, *38*, 357. (b) Alemán, C.; Puiggalí, J. *J. Org. Chem.* **1995**, *60*, 910. (c) Benedetti, E.; Pedone, E. M.; Kawahata, N. H.; Gooman, M. *Biopolymers* **1995**, *36*, 659. (d) Alemán, C. *Proteins* **1997**, *29*, 575.
- (2) (a) Chorev, M.; Shavitz, R.; Goodman, M.; Minick, S.; Guillemin, R. *Science* **1979**, *204*, 1210. (b) Verdini, A. S.; Silvestri, S.; Becherucci, C.; Longobardi, M. G.; Parente, L.; Peppoloni, S.; Perretti, M.; Pileri, P.; Pironi, M.; Viscomi; Nencioni, L. *J. Med. Chem.* **1991**, *34*, 3372. (c)

- Nishikawa, N.; Komazawa, H.; Orikasa, A.; Yoshikane, M.; Yamaguchi, J.; Kojima, M.; Ono, M.; Itoh, I.; Azuma, I.; Fujii, H.; Murata, J.; Saiki, I. *Bioorg. Med. Chem. Lett.* **1996**, *6*, 2725–2728. (d) Chorev, M.; Goodman, M. *Trends Biotechnol.* **1995**, *13*, 438–445.
- (3) Marraud, M.; Dupont, V.; Grand, V.; Zerkout, S.; Lecoq, A.; Boussard, G.; Collet, A.; Aubry, A. *Biopolymers* **1993**, *33*, 1135.
- (4) Fletcher, M. D.; Campbell, M. M. *Chem. Rev.* **1998**, *98*, 763.
- (5) (a) Guichard, G.; Muller, S.; van Regenmortel, M.; Briand, J. P.; Mascagni, P.; Giral, E. *Trends Biotechnol.* **1996**, *14*, 44. (b) Chorev, M.; Goodman, M. *Trends Biotechnol.* **1996**, *14*, 43.
- (6) Wermuth, J.; Goodman, S. L.; Jonczyk, A.; Kessler, H. *J. Am. Chem. Soc.* **1997**, *119*, 1328.
- (7) (a) Stern, P. S.; Chorev, M.; Goodman, M.; Hagler, A. T. *Biopolymers* **1983**, *22*, 1885. (b) Stern, P. S.; Chorev, M.; Goodman, M.; Hagler, A. T. *Biopolymers* **1983**, *22*, 1901.
- (8) (a) Alemán, C.; Pérez, J. J. *THEOCHEM* **1993**, 285, 227. (b) Sandrone, G.; Dixon, D. A.; Hay, B. P. *J. Phys. Chem. A* **1999**, *103*, 3554.
- (9) Alemán, C.; Pérez, J. J. *THEOCHEM* **1994**, 304, 17.
- (10) Alemán, C.; Navarro, E.; Puiggalí, E. *J. Org. Chem.* **1995**, *60*, 6135.
- (11) Navarro, E.; Alemán, C.; Puiggalí, J. *Macromolecules* **1998**, *31*, 408.
- (12) Navarro, E.; Alemán, C.; Puiggalí, E. *J. Am. Chem. Soc.* **1995**, *117*, 7307.
- (13) (a) Wu, Y.-D.; Wang, D. P. *J. Am. Chem. Soc.* **1998**, *120*, 13485. (b) Alemán, C.; León, S. *THEOCHEM* **2000**, in press.
- (14) Alemán, J. J.; Pérez, J. J. *Int. J. Pept. Protein Res.* **1994**, *43*, 258.
- (15) Alemán, C. *J. Biomol. Struct. Dyn.* **1996**, *14*, 193.
- (16) McGregor, M. J.; Suhail, I. A.; Sternberg, J. E. *J. Mol. Biol.* **1987**, *198*, 295.
- (17) Kemme, A. A.; Shvets, A. E.; Bleidelis, J.; Ancans, J. E.; Cipens, G. I. *J. Struct. Chem. (Engl. Transl.)* **1976**, *17*, 965.
- (18) Mishnev, A.; Bleidelis, J. J.; Ancans, J. E.; Cipens, G. I. *J. Struct. Chem. (Engl. Transl.)* **1982**, *23*, 252.
- (19) El Masdouri, L.; Aubry, A.; Gomez, E.; Vitoux, B.; Marraud, M. *Acta Crystallogr., Sect. C* **1992**, *48*, 175.
- (20) El Masdouri, L.; Aubry, A.; Gomez, E.; Vitoux, B.; Marraud, M. *Acta Crystallogr., Sect. C* **1992**, *48*, 178.
- (21) Perczel, A.; Ángyan, J. G.; Kajtár, M.; Viviani, W.; Rivail, J.-L.; Marcoccia, J.-F.; Csizmadia, I. G. *J. Am. Chem. Soc.* **1991**, *113*, 6256.
- (22) Hariharan, P. C.; Pople, J. A. *Theor. Chim. Acta* **1973**, *23*, 213.
- (23) Möller, C.; Plesset, M. S. *Phys. Rev.* **1934**, *46*, 618.
- (24) (a) Miertus, S.; Scrocco, E.; Tomasi, J. *Chem. Phys.* **1981**, *55*, 117. (b) Miertus, S.; Tomasi, J. *Chem. Phys.* **1982**, *65*, 239.
- (25) Frisch, M. J.; Trucks, G. W.; Schlegel, H. B.; Scuseria, G. E.; Robb, M. A.; Cheeseman, J. R.; Zakrzewski, V. G.; Montgomery, Jr.; Stratmann, R. E.; Burant, J. C.; Dapprich, S.; Millam, J. M.; Daniels, A. D.; Kudin, K. N.; Strain, M. C.; Farkas, O.; Tomasi, J.; Barone, V.; Cossi, M.; Cammi, R.; Mennucci, B.; Pomelli, C.; Adamo, C.; Clifford, S.; Ochterski, J.; Petersson, G. A.; Ayala, P. Y.; Cui, Q.; Morokuma, K.; Malick, D. K.; Rabuck, A. D.; Raghavachari, K.; Foresman, J. B.; Cioslowski, J.; Ortiz, J. V.; Baboul, A. G.; Stefanov, B. B.; Liu, G.; Liashenko, A.; Piskorz, P.; Komaromi, I.; Gomperts, R.; Martin, R. L.; Fox, D. J.; Keith, T.; Al-Laham, M. A.; Peng, C. Y.; Nanayakkara, A.; Gonzalez, C.; Challacombe, M.; Gill, P. M. W.; Johnson, B.; Chen, W.; Wong, M. W.; Andres, J. L.; Gonzalez, C.; Head-Gordon, M.; Replogle, E. S.; Pople, J. A. *Gaussian 98, Revision A.7*; Gaussian, Inc.: Pittsburgh, PA, 1998.
- (26) Viviani, W.; Rivail, J.-L.; Perczel, A.; Csizmadia, I. G. *J. Am. Chem. Soc.* **1993**, *115*, 8321.
- (27) Gellman, S. H.; Dado, G. P.; Liang, G.-B.; Adams, B. R. *J. Am. Chem. Soc.* **1991**, *113*, 1164.
- (28) (a) Császár, A. G. *J. Mol. Struct.* **1995**, *346*, 141. (b) Császár, A. G. *J. Am. Chem. Soc.* **1992**, *114*, 9569. (c) Böhm, H.-J.; Brode, S. *J. Am. Chem. Soc.* **1991**, *113*, 7129. (d) Rommel-Möhle, K.; Hofmann, H.-J. *J. Mol. Struct.* **1993**, *285*, 211. (e) Gould, I. R.; Cornell, W. D.; Hillier, I. H. *J. Am. Chem. Soc.* **1994**, *116*, 9250. (f) Endredi, G.; Perczel, A.; Farkas, O.; McAllister, M. A.; Csonka, G. I.; Ladik, J.; Csizmadia, I. G. *J. Mol. Struct.* **1997**, *391*, 15. (g) Möhle, K.; Gussmann, M.; Rost, A.; Cimiraglia, R.; Hofmann, H.-J. *J. Phys. Chem. A* **1997**, *101*, 8571. (h) Frey, R. F.; Coffin, J.; Newton, S. Q.; Ramek, M.; Cheng, V. K. W.; Momany, F. A.; Schafer, L. *J. Am. Chem. Soc.* **1992**, *114*, 5369.